Supporting Information

Reddy et al. 10.1073/pnas.1415466112

SI Experimental Procedures

Coimmunoprecipitation and Mass Spectrometric Identification. *P. falciparum* 3D7 blood stage parasites were cultured in vitro according to methods as described earlier (1). Tightly synchronized schizont-stage parasites (44–48 h) were harvested by centrifugation at 2,000 × *g* for 5 min. The pellet was incubated in 0.15% saponin to lyse the erythrocytes.

Immunoprecipitation was performed as prescribed by the Pierce cross-link IP kit (ThermoFisher Scientific). The saponin-treated parasites were lysed and spun at 15,000 × g. The schizont-stage lysate was precleared with Protein G Sepharose beads for 2 h at room temperature. Thereafter, 2 mg of the precleared schizont lysate was incubated with 10 μL of Protein G Sepharose (GE Healthcare) that had been cross-linked with the antibody of interest. The Protein G Sepharose beads were then washed and eluted.

The peptides obtained after trypsin (Promega) digestion were analyzed by mass spectrometry. Tandem mass spectrometry experiments were performed on a hybrid Orbitrap Velos Pro mass spectrometer (ThermoFisher Scientific) using the Xcalibur version 2.1 coupled to a Nano LC-1000 HPLC nanoflow system via nanoelectrospray ion source. The trypsin digested samples were loaded on a precolumn (Acclaim PepMap100: 75 μm × 2 cm, C-18, 3 μm, 100 Å) that was further connected with an analytical column (Acclaim PepMap RSLC: 50 μm × 15cm, C-18, 2 μm, 100 Å). The peptides were eluted from the column with a gradient of 5% solvent B (solvent A: 5% acetonitrile in 0.1% formic acid; solvent B: 95% acetonitrile in 0.1% formic acid) to 90% solvent B over a period of 120 min with a flow rate of 300 nL/min.

The proteins were identified by blasting the peptides over a *P. falciparum* database (Uniprot), using Proteome Discoverer 1.4 (ThermoFisher Scientific) using the SEQUEST algorithm with a mass tolerance of 20 ppm for MS and 0.1 Da for MS/MS. A maximum of two missed tryptic cleavage sites was allowed. Carboxy-amido-methylation of cysteines was specified as a fixed modification. The peptide matches were validated using Percolator available with the Proteome Discoverer 1.4. We accepted peptides with a false discovery rate of 1%.

Mass spectrometry is a sensitive technique that may identify up to hundreds of proteins from a single immunoprecipitation elute. We considered only those proteins for which at least two unique peptides could be detected. However, the majority of the proteins are nonspecific bound protein contaminants (2). To filter these nonspecifically bound proteins, we used the corresponding preimmune IgGs as a negative control. The proteins pulled down by the preimmune antibodies were treated as background and were removed from the list of proteins that were immunoprecipitated by the immune IgGs. In our immunoprecipitation experiments, we consistently detected PfRH5, PfRipr, and CyRPA to be specifically immunoprecipitated by the PfRH5, PfRipr, and CyRPA immune IgGs, with significantly higher scores in comparison with other additional low scoring background proteins that were primarily detected in only one experiment and not reproducible.

Recombinant Protein Expression and Purification. Two DNA fragments of CyRPA (CyRPA-1: 29–208 amino acids; and CyRPA-2: 209–362 amino acids) were PCR amplified from genomic DNA (3D7) with the following primers: CyRPA-1 (Fwd: 5′-TGTGTGgctagcCGTCATGTTTTTATAAGGACT-3′; Rev: 5′-TGTGTGctcgagCCATGTCTCGCCTTTGT-3′) and CyRPA-2 (Fwd: 5′-TGTGTGgctagcACCAAAATAGTCATAAAATATGA-3′; Rev: 5′-TGTGTGctcgagCTCATAGTTAGCATAGTATA-3′). The DNA fragment corresponding to the full-length protein CyRPA-FL (29–362 amino acids) excluding the N-terminal signal sequence was amplified using these primers: Fwd: 5′-TGTGTGgctagcCGTCATGTTTTTATAAGGACT-3′; Rev: 5′-TGTGTGctcgagCTCATAGTTAGCATAGTATA-3′ from cDNA, which had been prepared from 3D7 total RNA using the single-strand cDNA synthesis kit (Life Technologies). The respective DNA fragments were digested with the NheI/XhoI restriction enzymes and further cloned in theT7 promoter based pET-24b expression vector (Novagen) to yield the plasmids pCyRPA1-pET24b, pCyRPA2-pET24b, and pCyRPA-FL-pET24b.

Similarly, two fragments of PfRipr corresponding to the EGF-like domains present at both the amino terminus (Ripr-1) and carboxyl-terminus (Ripr-2) were selected for expression as recombinant proteins. DNA fragments for both protein constructs were PCR-amplified from genomic DNA (3D7) using the following primers: Ripr-1 (Fwd: 5′-GTACATTTACTAcatatgGTATATAATGATGATACACATAAAGCAACAT-3′; Rev: 5′-CCGctcgagTTGATATAAATTATTTTTATAAAATTTTTCT TTTTTATGTGGTTC-3′) and Ripr-2 (Fwd: 5′-CGCTAGCTACTAcatatgAATGAAGAAACAGATATTGTAAAAT-3′; Rev: 5′-CCGctcgagATCTTCTAAAACACATTTTC C-3′). The respective DNA fragments were digested with the NdeI/XhoI restriction enzymes and cloned in the pET-24b expression vector to yield the plasmids pRipr1-pET24b and pRipr2-pET24b.

All protein constructs were expressed in BL21(DE3) *E. coli* cells. *E. coli* BL21(DE3) cells were transformed with each of the five plasmids and used for production of the respective recombinant proteins. Transformed *E. coli* BL21(DE3) were cultured in Luria Bertani broth at 37 °C and later induced with 1 mM isopropyl β-D-1-thiogalactopyranoside when the OD_{600} was approximately 0.8–0.9. Cells were harvested by centrifugation at 3,000 × g, after 4 h of induction at 37 °C. Cell pellets were lysed by sonication, and the recombinant proteins were analyzed for their expression.

Except Ripr-2 that was expressed in the soluble fraction, all of the recombinant proteins (CyRPA-1, CyRPA-2, CyRPA-FL, Ripr-1) were expressed as inclusion bodies. Harvested pellets (inclusion bodies) obtained after cell lysis were washed extensively and solubilized in a denaturing buffer [10 mM Tris, 100 mM $Na_2HPO_4.7H_20$, 10 mM imidazole, 0.25 M NaCl, 1 mM β-mercaptoethanol, and 6 M guanidine·HCl (pH 8.0)]. The clarified supernatants obtained after centrifugation of the solubilized inclusion bodies were applied to a preequilibrated Ni-NTA agarose column (Qiagen) to purify the proteins of interest by immobilized metal affinity chromatography (iMAC) using an imidazole gradient. The iMAC-purified denatured proteins were refolded in redox conditions by rapid dilution (30-fold) in a Tris-based buffer (pH 8.0) comprising 1 mM GSH (reduced glutathione) and 0.1 mM GSSG (oxidized glutathione). The recombinant proteins were further purified to homogeneity using anion exchange and SEC and stored in PBS. Ripr-2 was expressed in the soluble fraction. The supernatant collected after cell lysis was then purified by immobilized metal affinity chromatography (Ni-NTA, G Biosciences). Ripr-2 was further purified to homogeneity by passing it over an anion-exchange and SEC. The identity of the recombinant proteins was confirmed by LC-MS, as well as by immunoblotting using anti-HIS antibodies.

Animal Immunization and Antibody Generation. For the animal experiments, the animals' care was in accordance with institutional guidelines. Animal immunization and total IgG purification were done as reported previously (3, 4). Briefly, mice

and rats were immunized intramuscularly with 25 μg and 50 μg of the recombinant proteins (CyRPA and PfRipr), respectively. The proteins were emulsified with complete Freund's adjuvant (Sigma) on day 0 immunization, followed by two boosts emulsified with incomplete Freund's adjuvant on day 28 and 56. The sera were collected on day 70. Antibody levels were measured by ELISA. Total IgG was purified from the rat sera using a Protein G affinity column (GE Healthcare), dialyzed with iRPMI, and used in invasion inhibition assays. PfRH5 antibodies have been described recently and were used from that study (3).

Western Blot Analysis of the Immunoprecipitated Elutes. Both the immune as well as the corresponding preimmune sera were used to perform the immunoprecipitation experiments. Elutes were run on SDS/PAGE and transferred to a nitrocellulose membrane. Immunoblot analysis was performed using antibodies from a distinct species than that used for immunoprecipitation.

Immunofluorescence Staining of Schizont-Stage Parasites. Schizont-stage parasites fixed in prechilled methanol (−20 °C) were air-dried and blocked using 3% BSA in PBS for 2 h at room temperature (~25 °C). Slides were incubated at room temperature (~25 °C) for 1 h with different antibodies at the following dilutions: anti-rPfRH5 rabbit sera (1:100); anti-PfRH2 rabbit sera (1:50); anti-CyRPA mouse sera (1:50); anti-PfRipr-2 mouse sera (1:50); anti-EBA-175 rat sera (1:50); anti-PfRipr-2 rat sera (1:50). Slides were then washed and incubated with secondary antibodies conjugated with Alexa Fluor 488/Alexa Fluor 594. The slides were washed and mounted in ProLong Gold antifade reagent with DAPI (Invitrogen) and were viewed on a superresolution confocal microscope (*N*-SIM, Nikon). The images were processed using Nikon NIS Elements AR 4.13.04 software.

Ion-Exchange and SEC Analysis of the Native PfRH5/PfRipr/CyRPA Parasite Multiprotein Complex. Saponin-treated schizont pellets were lysed in lysis buffer containing 25 mM Tris (pH 7.4), 150 mM NaCl, 1 mM EDTA, 1% Nonidet P-40, and 5% (vol/vol) glycerol. The lysate obtained was diluted 10-fold in TBS (pH-7.5) and then loaded onto a Q-Sepharose column (GE Healthcare). The column was washed in TBS, and then elution was attempted using a stepwise gradient of NaCl. The three peaks obtained at 350, 500, and 750 mM NaCl were collected separately and analyzed for the presence of the antigens by immunoblotting.

The 350 mM ion-exchange fraction was loaded onto an SEC-200 column (SEC, GE Healthcare). The eluted protein fractions (1.5 mL each) were analyzed by immunoblotting for the presence of each antigen. To demarcate the size of the PfRH5/PfRipr/CyRPA complex, standard molecular weight markers (Sigma) were run on the SEC-200 column. Culture supernatants were prepared as described previously (5). The culture supernatant was dialyzed against TBS (pH 7.5), concentrated, and analyzed on an SEC-200 as discussed above.

BN-PAGE. Blue native Tris-histidine gels were run as described previously (6). Briefly, parasite proteins (schizont lysate or culture supernatant) were run on a 4–20% gel with a BN-PAGE dye containing Coomassie G-250 and further transferred on to a nitrocellulose membrane. The PfRH5/PfRipr/CyRPA complex was detected by immunoblotting using antibodies against the respective antigens.

Isolation of Invasive Merozoites and Immunofluorescence Analysis. Invasive merozoites were prepared as has been reported earlier (7). Briefly, synchronized mature segmented-stage parasites were allowed to rupture. The free merozoites were separated from the erythrocytes by centrifugation at 2,000 × *g* for 5 min. The supernatant collected were then spun at 4,000 × *g* to pellet the merozoites. The merozoites were then treated with 1 μM Cytochalasin D (Sigma Aldrich) for 5 min and then incubated for 10 min with erythrocytes. The sample was then washed twice with PBS to remove the free merozoites and then fixed in 0.0075% glutaraldehyde/4% (wt/vol) paraformaldehyde for 30 min at 4 °C. For the NapL (8) staining under permeabilizing conditions the glutaraldehyde/paraformaldehyde fixed samples were treated with 0.1% Triton X-100 for 15 min at 4 °C before staining.

Immunofluorescence staining was performed as has been discussed above. The primary antibodies for merozoite staining have been used at the following dilutions: anti-rPfRH5 rabbit sera (1:100); anti-NapL rabbit sera (1:50); anti-CyRPA mouse sera (1:50); anti-PfRipr-2 mouse sera (1:50); anti-PfRipr-2 rat sera (1:50); and anti-MSP-1_{19} rat sera (1:50). The images were captured using superresolution confocal microscope (*N*-SIM, Nikon). Three-dimensional reconstruction of the deconvolved Z-stacks was done using Imaris software version 6.4.2 (Bitplane scientific), as previously described (9).

Triton X-114 Partitioning Experiments. For the partitioning experiments (10, 11), schizont-stage parasites were lysed with 1% Triton X-114 in PBS (pH 7.4), layered over ice-cold 6% (wt/vol) sucrose, and further incubated at 37 °C for 5 min. The solution was spun (500 × *g*) for 5 min at 37 °C. The aqueous and the pellet fraction were collected, washed, mixed with 2× SDS running dye, and analyzed by immunoblotting.

Parasite Radiolabeling with GPI Precursors. Parasite radiolabeling was done as described previously (12, 13). Briefly, *P. falciparum* schizont stage (42–44 h) parasites were purified over a Percoll gradient and allowed to grow for 3 h in glucose-free RPMI 1640 supplemented with 10 mm fructose, 24 mM Hepes, 0.36 mM hypoxanthine, and 24 mM sodium bicarbonate in the presence of 50 μCi mL^{-1} d-[6-3H(N)]glucosamine hydrochloride and 50 μCi mL^{-1} d-[2-3H]mannose at 37 °C. The tritium labeled parasites were then harvested and lysed with 25 mM Tris (pH 7.4), 150 mM NaCl, 1 mM EDTA, 1% Nonidet P-40, and 5% (vol/vol) glycerol. The lysate was first precleared using Protein G Sepharose beads conjugated with the corresponding preimmune IgGs. The precleared lysate were then used to perform immunoprecipitation as described above. The detection of the radioactive signal was done as previously described (13).

Invasion Inhibition Assay. Single-cycle invasion inhibition assays were performed and evaluated as previously described (3, 4). For analyzing growth inhibition in a two-cycle assay, schizont-stage parasites at an initial parasitemia of 0.2% at 1% hematocrit were incubated with purified total IgG for two cycles (90 h) of parasite growth. After ~60 h of invasion, 10 μL of fresh media was added to each well. The parasite-infected erythrocytes were stained with ethidium bromide dye and measured by FACS as described previously (4). The percent invasion inhibition for immune IgG was calculated with respect to the control preimmune IgG from the same animal.

For assessing synergy, invasion inhibition was evaluated by varying the concentrations (0.5–4.0 mg/mL) of the purified total IgG against CyRPA, Ripr-1/Ripr-2 in the presence of a fixed concentration of anti-PfRH5 (1 mg/mL) IgG. Synergy will be an effect greater than predicted from the two agents, when mixed together, acting independently of each other to produce an additive effect. The predicted additive effect was calculated by the formula of Bliss additivity, as described previously (14).

The results represent the average of three independent experiments performed in duplicate, and the error bars represent the SEM. *P* values were calculated using two-tailed unpaired Students *t* test ($^{*}P \leq 0.05$; $^{**}P \leq 0.01$).

CyRPA Gene Knockout Strategy. To determine the functional significance of CyRPA for parasite survival, we attempted to disrupt the CyRPA genetic locus by double crossover homologous recombination. We used the pCC1 vector construct with positive and negative selection markers. pCC1 comprises hDHFR for positive selection and the *Saccharomyces cerevisiae* cytosine deaminase/uracil phosphoribosyl transferase (ScFCU) chimeric gene for negative selection that is driven by the heat shock protein 86 promoter (5′ hsp86) and flanked by the *Plasmodium berghei* dhfr terminator (3′ PbDT). To generate the pCC1 transfection vector construct, a 5′ fragment of the CyRPA gene was PCR amplified from *P. falciparum* 3D7 genomic DNA using the primer set 5′-GCCCGCGGTGGTTCCAAATATTAATTT-GAAAAAG-3′ (forward) and 5′-GCACTAGTATCCTTCTTT-CTATTTGAAAATTC-3′ (reverse) and further cloned upstream of the hDHFR cassette in the pCC1 vector using the restriction sites SacII and SpeI to produce the construct pCC1-CyRPA-5′. The 3′ fragment of the CyRPA gene loci was PCR amplified using the primer set 5′-GCGAATTCAAGAATGTTAATTTTATTGAGT GTA-3′ (forward) and 5′-GCCCATGGATAATACCAATTTGT-CTACATTCA-3′ (reverse) and cloned downstream of the hDHFR cassette in pCC1-CyRPA-5′ construct using restriction sites EcoRI and NcoI to produce the construct pCC1-CyRPA. Synchronized *P. falciparum* 3D7 ring stage parasites were transfected with 100 μM of purified plasmid DNA (Qiagen) by electroporation (310 V, 950 mF), and the transfected parasites were subjected to 2.5 nM of WR99210 drug selection. However, after repeated attempts we were unable to obtain any viable parasites, suggesting that the CyRPA gene is essential for the parasite.

1. Trager W, Jensen JB (1976) Human malaria parasites in continuous culture. *Science* 193(4254):673–675.
2. Huang BX, Kim HY (2013) Effective identification of Akt interacting proteins by two-step chemical crosslinking, co-immunoprecipitation and mass spectrometry. *PLoS ONE* 8(4):e61430.
3. Reddy KS, et al. (2014) Bacterially expressed full-length recombinant *Plasmodium falciparum* RH5 protein binds erythrocytes and elicits potent strain-transcending parasite-neutralizing antibodies. *Infect Immun* 82(1):152–164.
4. Pandey AK, et al. (2013) Identification of a potent combination of key *Plasmodium falciparum* merozoite antigens that elicit strain-transcending parasite-neutralizing antibodies. *Infect Immun* 81(2):441–451.
5. Gaur D, et al. (2007) Recombinant *Plasmodium falciparum* reticulocyte homology protein 4 binds to erythrocytes and blocks invasion. *Proc Natl Acad Sci USA* 104(45): 17789–17794.
6. Niepmann M, Zheng J (2006) Discontinuous native protein gel electrophoresis. *Electrophoresis* 27(20):3949–3951.
7. Singh S, Alam MM, Pal-Bhowmick I, Brzostowski JA, Chitnis CE (2010) Distinct external signals trigger sequential release of apical organelles during erythrocyte invasion by malaria parasites. *PLoS Pathog* 6(2):e1000746.
8. Chandra BR, Olivieri A, Silvestrini F, Alano P, Sharma A (2005) Biochemical characterization of the two nucleosome assembly proteins from *Plasmodium falciparum*. *Mol Biochem Parasitol* 142(2):237–247.
9. Riglar DT, et al. (2011) Super-resolution dissection of coordinated events during malaria parasite invasion of the human erythrocyte. *Cell Host Microbe* 9(1):9–20.
10. Ko YG, Thompson GA, Jr (1995) Purification of glycosylphosphatidylinositol-anchored proteins by modified triton X-114 partitioning and preparative gel electrophoresis. *Anal Biochem* 224(1):166–172.
11. Wang L, Coppel RL (2002) Triton X-114 phase partitioning for antigen characterization. *Methods Mol Med* 72:581–585.
12. Naik RS, et al. (2000) Glycosylphosphatidylinositol anchors of *Plasmodium falciparum*: Molecular characterization and naturally elicited antibody response that may provide immunity to malaria pathogenesis. *J Exp Med* 192(11):1563–1576.
13. Hinds L, Green JL, Knuepfer E, Holder AA, Grainger M (2009) Novel putative glycosylphosphatidylinositol-anchored micronemal antigen of *Plasmodium falciparum* that binds to erythrocytes. *Eukaryot Cell* 8(12):1869–1879.
14. Williams AR, et al. (2012) Enhancing blockade of *Plasmodium falciparum* erythrocyte invasion: Assessing combinations of antibodies against PfRH5 and other merozoite antigens. *PLoS Pathog* 8(11):e1002991.

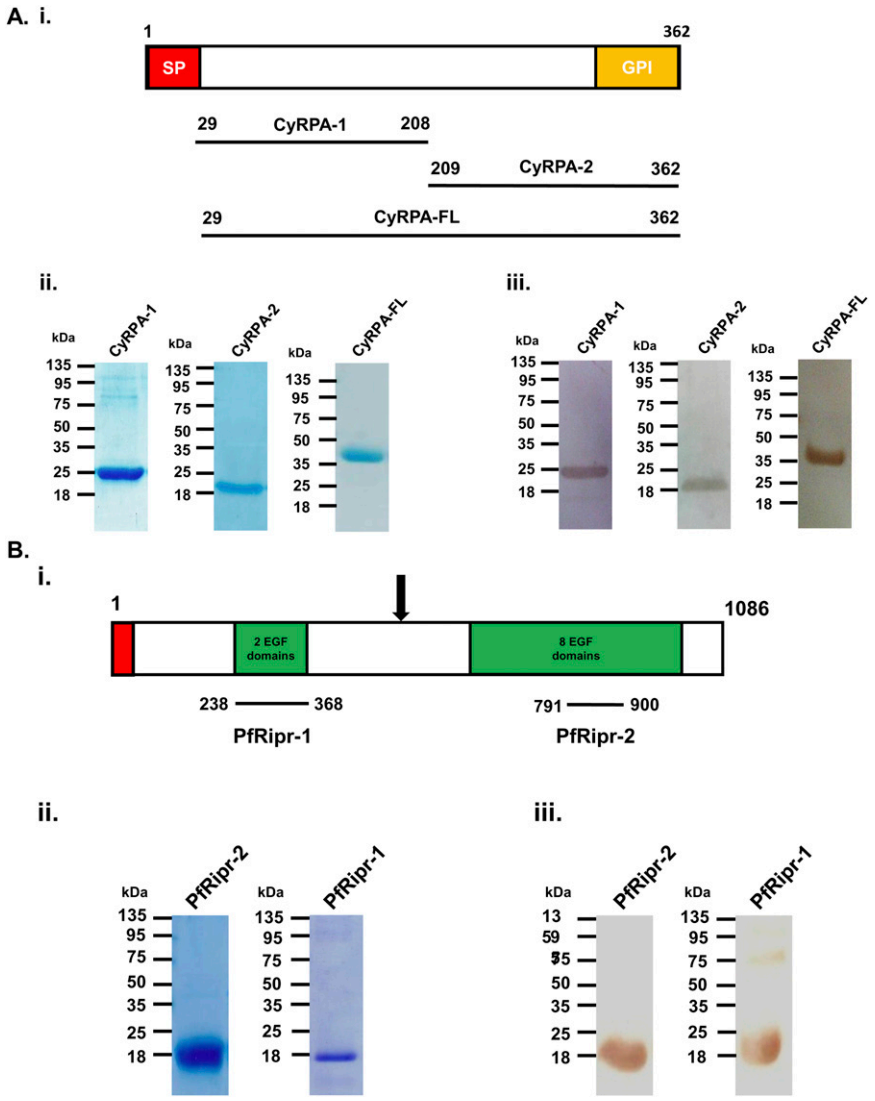

Fig. S1. Generation of CyRPA and PfRipr recombinant protein constructs. (*A*, *i*) Diagram shows the characteristics of CyRPA and the regions used to generate the recombinant proteins. CyRPA contains a predicted N-terminal signal peptide (1–28 amino acids). We generated recombinant proteins corresponding to full-length CyRPA-FL (29–362 amino acids), CyRPA-1 (29–208 amino acids), and CyRPA-2 (209–362 amino acids). The GPI site has been experimentally confirmed in this report. (*A*, *ii*) SDS/PAGE gels showing the purified recombinant proteins. (*A*, *iii*) Anti-HIS antibodies detected the recombinant proteins in immunoblots confirming the presence of the C-terminal His-tag. (*B*, *i*) PfRipr contains a signal peptide and cysteine-rich EGF-like domains (two at the N terminus and eight toward the C terminus). We produced recombinant proteins: PfRipr-1 corresponding to amino acids 238–368 (two N-terminal EGF-like domains) and PfRipr-2 corresponding to amino acids 791–900 comprising two among eight EGF-like domains toward the C terminus. (*B*, *ii*) SDS/PAGE gels showing the purified recombinant proteins. (*B*, *iii*) Anti-HIS antibodies detected the recombinant proteins in immunoblots confirming the presence of the C-terminal His-tag.

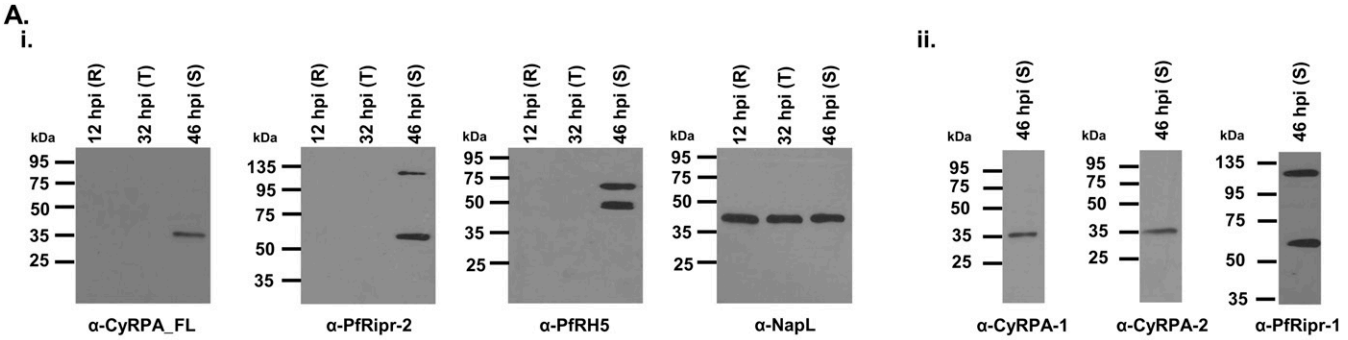

B.

IP-CyRPA

Gene ID	Scores	Protein	Plasmodb ID
O97302	97.5, 99.1	PfRipr	Pf3D7_0323400
Q8IFM5	67.5, 89.6	PfRH5	Pf3D7_0424100
Q8IFM8	58.4, 68.7	CyRPA	Pf3D7_0423800

IP-PfRipr

Gene ID	Scores	Protein	Plasmodb ID
O97302	164, 189.3	PfRipr	Pf3D7_0323400
Q8IFM5	133, 133.9	PfRH5	Pf3D7_0424100
Q8IFM8	82, 124	CyRPA	Pf3D7_0423800

C.

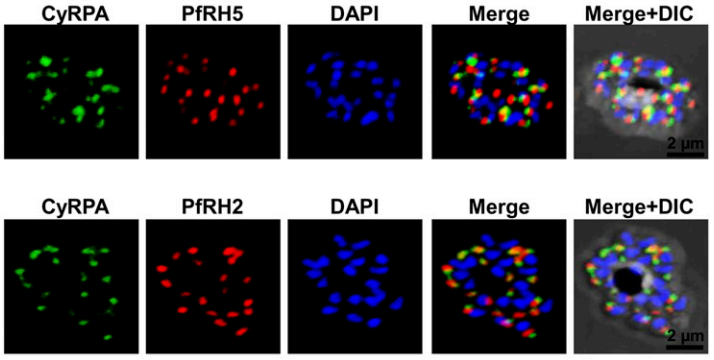

Fig. S2. PfRH5, PfRipr, and CyRPA proteins interact to form a multiprotein complex. (*A*) Specificity of the antibodies generated against the recombinant proteins. (*A*, *i*) CyRPA, PfRipr-2, and PfRH5 antibodies detected the expression of the corresponding native parasite proteins only in the schizont-stage parasites. CyRPA antibodies detected a 35-kDa parasite protein band, whereas PfRipr-2 antibodies detected the full-length (123 kDa) and a processed (60-kDa) band. PfRH5 antibodies detected both the full-length 63-kDa and 45-kDa processed proteins. Expression of NapL (nucleosome assembly protein L) was analyzed as a loading control as reported earlier (8). (*A*, *ii*) CyRPA-1, CyRPA-2, and PfRipr-1 antibodies also detected the corresponding native parasite proteins in the schizont-stage parasites (*hpi, hours post invasion; [R] Ring, [T] Trophozoite, and [S] Schizont). (*B*) Mass spectrometric analysis of proteins coimmunoprecipitated by anti-CyRPA and anti-PfRipr2 antibodies detected PfRH5-PfRipr and PfRH5-CyRPA, respectively, confirming the three proteins as interacting partners. The scores represent the values obtained in the two independent experiments. (*C*) CyRPA does not colocalize with the Rhoptry neck (PfRH2) and Rhoptry bulb (PfRH5) proteins. (Scale bar, 2 μm.)

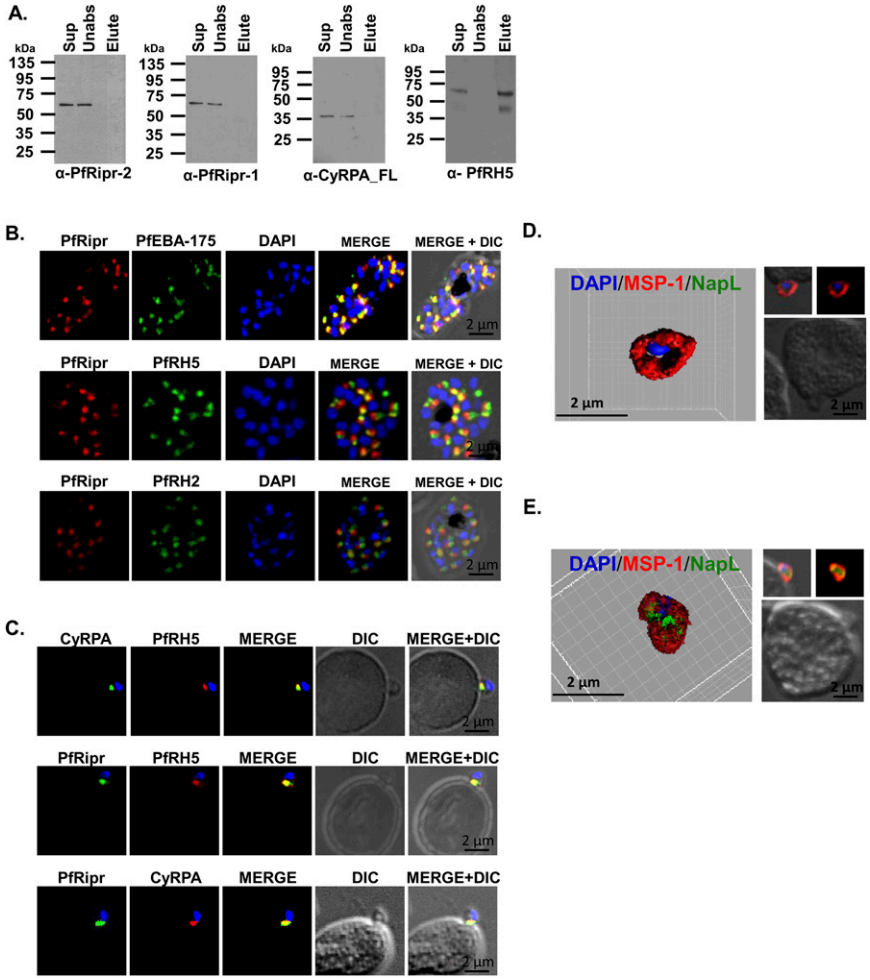

Fig. S3. CyRPA and PfRipr lack erythrocyte binding activity but colocalize with PfRH5 on the merozoite surface. (*A*) PfRipr and CyRPA do not bind erythrocytes because they were not detected among the proteins eluted from the erythrocyte (elute fraction) but detected in the unabsorbed fraction representing the proteins that did not bind with the erythrocyte (Unabs). PfRH5 was detected in the elute fraction and not in the unabsorbed fraction (Unabs). They probably dissociate during the PfRH5-Basigin interaction. Sup, culture supernatant; Unabs, culture supernatant after adsorption with erythrocytes; Elute, proteins eluted from the adsorbed erythrocyte. (*B*) PfRipr is localized in the micronemes in schizont-stage parasites. PfRipr-2 antibodies recognize PfRipr to colocalize with micronemal proteins (EBA-175) but not with the rhoptry proteins (PfRH2, PfRH5). (*C*) PfRH5, PfRipr, and CyRPA colocalized on the apical surface of an invading merozoite, indicating that the PfRH5/PfRipr/CyRPA complex is formed at the merozoite surface. (*D*) As a control, staining of a cytosolic parasite protein NapL (nucleosome assembly protein L) (8) was not detected under the nonpermeable fixing conditions using glutaraldehyde/paraformaldehyde, suggesting that the fluorescent signals were obtained only from surface localized proteins. (*E*) NapL staining could only be visualized when the glutaraldehyde/paraformaldehyde fixed parasites were permeabilized by 0.1% Triton X-100. MSP-1 staining remained unaffected under both permeabilized and nonpermeabilized conditions. (Scale bar, 2 μm.)

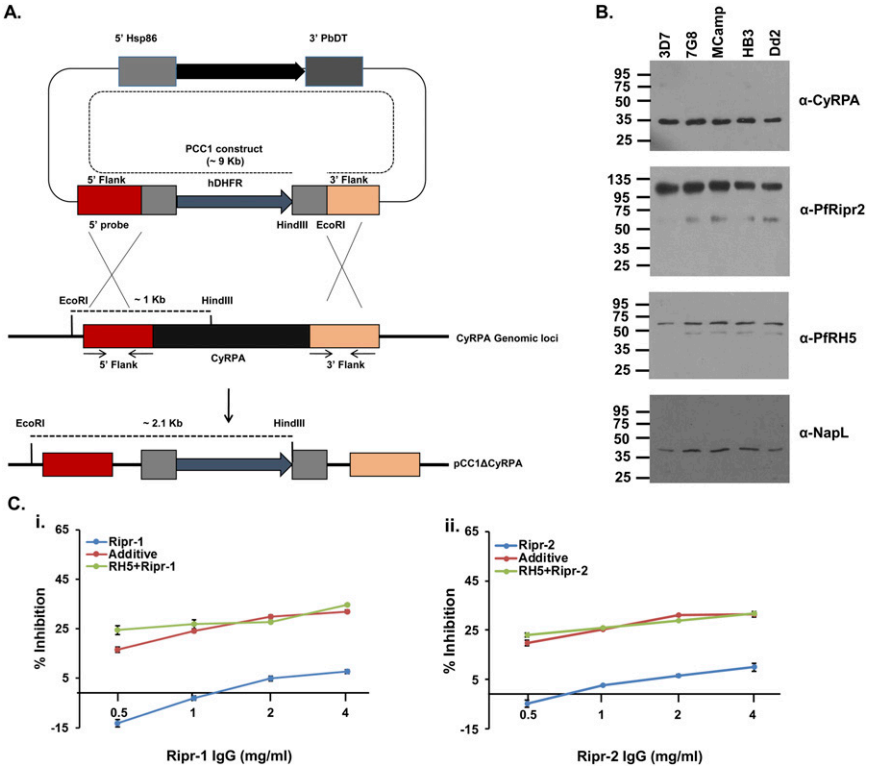

Fig. S4. PfRH5-Ripr-CyRPA complex is essential for invasion. (*A*) Strategy to genetically disrupt the CyRPA gene and expression analysis of the PfRH5, PfRipr, and CyRPA proteins among *P. falciparum* strains. Diagram showing the pCC1-construct based CyRPA gene knockout strategy. hDHFR cassette is flanked by 5′ and 3′ ends of the CyRPA gene. Genomic loci before and after homologous recombination are depicted. Location of the restriction sites, probe, and fragment sizes predicted to be detected by Southern blotting are shown. (*B*) PfRH5, PfRipr, and CyRPA expression was detected in five *P. falciparum* worldwide strains that differ in their invasion phenotypes and display differential expression of PfRH-1/-2/-4 proteins. (*C*) Invasion inhibition efficacy of PfRipr-1 and PfRipr-2 antibodies in combination with PfRH5 antibodies. PfRipr-1 (*C*, *i*) and PfRipr-2 (*C*, *ii*) antibodies alone were not efficient in inhibiting erythrocyte invasion (blue curve). In presence of a fixed concentration of anti-PfRH5 antibodies (1 mg/mL total IgG), the invasion inhibitory activity of PfRipr-1 and PfRipr-2 antibodies was tested (green curve). The red curve is a theoretical curve that represents the invasion inhibitory activity predicted by Bliss additivity (14). The anti-PfRH5 IgGs when tested alone at 1.0 mg/mL gave an invasion inhibition of 26.27(±2.17). No significant additive increase in invasion inhibition was observed in the presence of 1 mg/mL of anti-PfRH5 antibodies. The error bars represent the SEM of three independent experiments performed in duplicate.

Dataset S1. List of proteins detected by mass spectrometric analysis after immunoprecipitation experiments by both immune and preimmune antibodies

Dataset S1